Integrated Ferroelectrics ›
An International Journal
Volume 205, 2020 - Issue 1: Proceedings of the International Conference on Nano-Structured Materials and Devices (ICNSMD-2018): Part IV of IV

Dispersion and Optical Activities of Copper (II) Metal Oxide Nanoparticles with Polyethylene Glycol in Aqueous Medium Studied with Physicochemical Properties and UV-Vis Spectrophotometry

Salama A. Yaseen, Ahmed S. Alameen, Faizaa A. Saif, Sachin. B. Undre, P. W. Khirade & Prabhakar B. Undre

Pages 131-145 | Received 01 Oct 2018, Accepted 12 Aug 2019, Published online: 09 Feb 2020

Cite this article https://doi.org/10.1080/10584587.2019.1675009 Check for updates

Abstract

Copper (II) oxide nanoparticles are considered to be transition metal oxide having unique properties and could be useful in biochemical and biomedical applications. The hydrophilic Σ Settings ompatible polyethylene glycols (PEG) were used for dispersion of CuO in aqueous medium. The physicochemical properties (PCPs) and absorbance were determined for CuO dispersed. The PCPs and optical data showed a maximum CuO dispersion with water and PEG which

dispersion activities The results can provide new insights in the development of dispersion activities of CuO with PEG (400 and 6000).

Keywords: Copper oxide nanoparticles PEG biocompatible polymer dispersion activities physicochemical properties

1. Introduction

The dispersion of metal oxide nanoparticles (MONPs) in the form of dry powders in a liquid phase have attracted significant due to their potential applications in the field of ceramic, biochemical, biomedical, coating technology and materials sciences [1–4]. Thus, during of the last decade, the MONPs have interesting study due to the exceptional structural properties useful for developing a various application in field of nanotechnology and nanomedicine [5]. The copper oxide nanoparticles (CuO NPs) have extensively attracted for fundamental and practical reasons and widely exploited for diverse applications therefore, it can be useful in industry and other applications [6]. The Cupric oxide or copper oxide (CuO), is a semiconductor (p-type) with a bandgap of 1.0–1.9 eV [7].

The CuO nanoparticles have wide range of application in variety area as magnetic storage media, gas sensors [6], fuel cells [8], lithium batteries and electrochemical sensing [9], solar cells [4], antibacterial and antifungal [10] and many others. All this properties because of photoconductive, photochemical, optical and catalytic activity [11].

The effective mechanisms of CuO nanoparticles dispersed at different Reynolds numbers has been investigated to predict thermal entropy generation in dispersion system [12].The fast dissolution of CuO NPs release ions and make them toxic in nature and possess restrictions over to develop applications on human health, soil organisms and phytotoxic effects [13,14]. Hence, CuO NPs needs dispersion medium to overcome this restriction. The polyethylene glycol (PEG) is nonionic, linear polymer [13], and it has been widely utilized in the pharmaceutical and biomedical industries and biotechnical applications as medicine [15,16], drugs and Proteins [17]. The PEGs with molecular weights less than 700 have some of properties as slightly hazy, colorless, highly viscous and weak characteristic odor, while PEGs with high molecular weight

biocompatible polymer having unique properties and soluble in water (hydrophilic in nature) and most of the organic solvents. The PEG mixtures with water may provide substantially improved physicochemical properties (PCP) that can be used in different way of industrial and chemical applications [19]. Many researchers have been focused on the solutions of PEG and water used in purification and separation some of product which contain biomaterials, proteins, and enzymes [16, 20–24].

The present work is focused on hydrophilic and hydrophobic interactions between CuO and PEG in aqueous medium estimated from their PCPs and optical behavior studies. On the basis of solute-solvent dispersion or interactions PCPs were used to investigate dispersion with PEG to develop stable and efficient metal oxide based nanoparticles to develop potential applications in environmental, human health and catalytic reactions.

2. Experimental

2.1. Materials

Copper (II) oxide nanoparticles (Alfa Aesar), PEG_{400} (Merck, Germany), PEG_{6000} (Sigma-Aldrich) and water HPLC and spectroscopic grade (Molychem Company). All chemical which used without further purification.

2.2. Preparation of Dispersed Nanoparticles

The micro molar (μM) solutions of CuO NPs, PEG_{400} and PEG_{6000} ranging from (25 to 150 μM) with water were prepared. To determine CuO NPs dispersion activity, solution of CuO NPs in 150 μM PEG_{400} and PEG_{6000}, respectively, were prepared in the range (25–150 μM at an interval 25 μM) of CuO NPs and stirred 30 min at room temperature to obtain homogenous dispersion. Further, the solutions were sonicated for 30 min by Ultra-sonication which used to disperse agglomerates. The solutions were stored in sealed volumetric flask to avoid any kind of contamination and chemical reactions.

2.3. XRD Diffraction

The X-ray diffraction (XRD) patterns of the powdered samples were recorded using BRUKER

Scherrer equation. The data was collected with a step size of 0.00204470 in the 2θ range from 5° to 100°.

2.4. PCP Measurement

Density measurements were carried out using a 10 cm^3 glass pycnometer with error ±0.01. The pycnometer was filled with the solution. Densities were determined from measurements of the mass of the samples and the pycnometer volume. The volume of the pycnometer was calibrated using double-distilled water and further used for measurement. Refractive index for all samples were measured by Abbe Refractometer from BESTO.

2.5. Optical Properties Measurement

The SL-210 Multipurpose UV–Vis spectrophotometer was used to characterize the optical properties of the samples. Absorbance was measured in a 1 cm cuvette and spectra were recorded at room temperature with accuracy ± 0.5 nm. All pure samples, binary and ternary system are recorded in the wavelength ranges from 200 to 900 nm.

3. Results and Discussion

3.1. X-Ray Diffraction Analysis

The XRD peaks are located at angles (2θ°) of 32.54, 35.59, 38.80, 48.90, 53.50, 58.39, 61.60, 66.30, 72.46 and 75.13 indicated the formation of a type of monoclinic CuO NP structure as depicted in Figure 1. For confirm average crystalline size of the CuO NPs is calculated after appropriated related corrections from X-ray line broadening of the diffraction peaks using Debye–Scherer's equation for determine average crystalline size.

$$D = 0.94\,\lambda / \beta \cos \theta$$

where λ is the wavelength of X-ray used (0.154060 nm), β is the angular peak width at half maximum in radians and θ is Bragg's diffraction angle. The average crystalline size is estimated as 30.41 nm for CuO NPs whereas the size of CuO in the range (30–50) nm. The results confirm the nano range of CuO NPs.

In this article

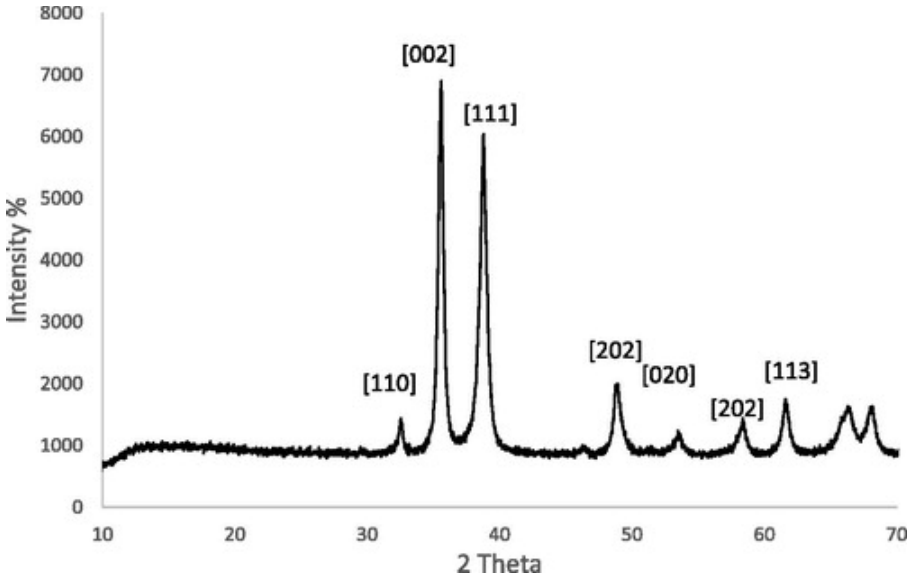

Display full size

3.2. PCP

The interaction or dispersion of the nanoparticles based on intermolecular interactions which could be determined with physicochemical characterization. The PCPs such as density, apparent molar volume, refractive index, molar refraction and pH were determined for the determination of the molecular interaction (MI) mechanism between the CuO NPs and PEG_{400}/PEG_{6000} separately. The intermolecular forces (IMF) which are generated through the MI between solute-solvent depend on the structural properties of substance present in the solutions. The PEG polymer having alkyl chain (hydrophobic characteristics) and [sbond]OH groups (hydrophilic characteristics) in their structural framework and could be accountable to initiate the intermolecular interactions with nanoparticles. The relative surface and structural activities of ([sbond]CH_2[sbond]CH_2)$_n$ and [sbond]OH along with their structure making or breaking actions on dispersion of CuO NPs are obtained from a comparison of density, apparent molar volume, refractive index, speed of light, molar refraction and pH. Hence, CuO NPs dispersion in aqueous medium which is facilitated by PEG_{400} and PEG_{6000} demonstrated through PCPs.

3.3. Density

Density is mass per unit volume, and attraction forces in the form of IMF that hold the molecules together through molecular interaction (MI). The density values found 1.001 kg m^{-3} for water and given in Table 1. The densities illustrate internal pressure of the copper oxide

In this article

$$\rho = \rho^{\circ} + S\rho\ m + S\rho' m^2 \quad (1)$$

Table 1. Density (ρ, $\pm 10^{-3}$ kg m^{-3}), refractive index (μ_{ri}, $\pm 10^{-3}$) and pH ($\pm 10^{-2}$) at 303.15 K

Download CSV Display Table

The ρ° is limiting density and S_ρ is 1st degree slope which depict state of solute–solvent and solute–solute interactions respectively [25]. Values of the density was obtained for the PEG_{400}-W, PEG_{6000}-W, CuO[sbond]W binary systems and CuO-PEG_{400}, CuO-PEG_{6000} ternary systems at *T* = 303.15 K are presented in Table 2 and Figure 2. The increased density by increasing concentration of CuO NPs with water, PEG_{400} and PEG_{6000} due to the establishing hydrophilic-hydrophilic interactions dominant over [sbond]OH and dipoles of water ($H^{\delta+}$[sbond]$O^{\delta-}$[sbond]$H^{\delta+}$). Lower density inferred the dominance of hydrophobic-hydrophobic interactions of alkyl chain of PEG_{400} and PEG $_{6000}$ with water. Further, this fact is responsible in case of CuO NPs in water, PEG_{400}-W and PEG_{6000}-W systems. The limiting density value found as PEG_{6000}-W > PEG_{400}-W due to the length of hydrophobic chain and hydrophilic groups in PEG_{6000} which develops strong interaction through hydrogen bond (HB) with $H^{\delta+}$-$O^{\delta-}$-$H^{\delta+}$ and generate high internal pressure as compared to PEG_{400} (Table 3, Figure 2).

Figure 2. Density of CuO, PEG400, PEG6000, CuO-PEG400 and CuO-PEG6000 in water.

In this article

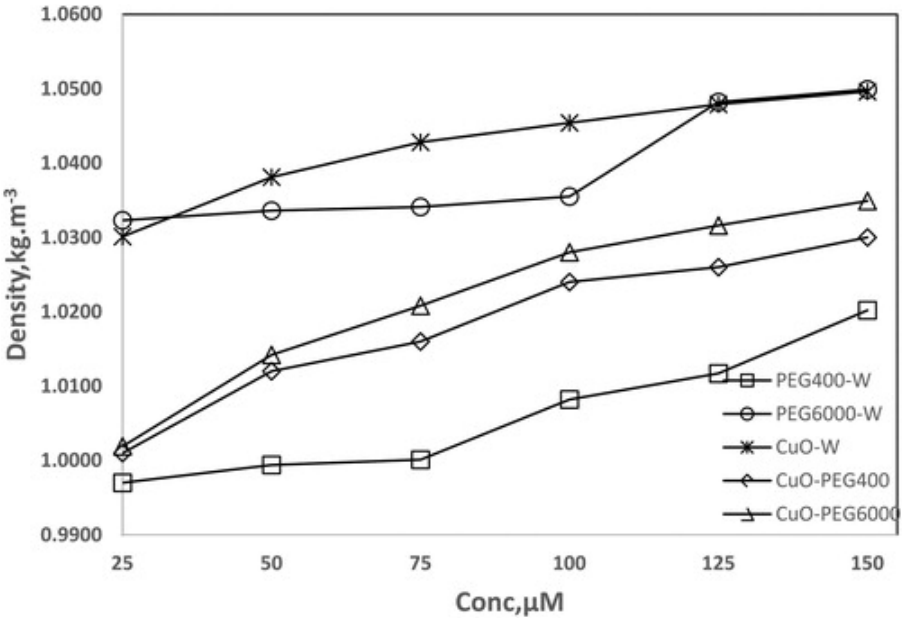

Display full size

Table 2: Micro molar (µM), density ($\rho \pm 10^{-3}$ kg m^{-3}), apparent molar volume ($V_\phi/10^{-2}$ m^3 mol^{-1}), refractive index (µri, $\pm 10^{-3}$), speed of light (C, $\pm 10^{-3}$, 10^8/ms^{-1}), molar refraction (R, $\pm 10^{-2}$ cm^{3}mol^{-1}), pH ($\pm 10^{-2}$) and absorbance (A, $\pm 10^{-3}$) at λmax 207, 268, 269, 273 and 265 nm of PEG400, PEG6000, CuO, CuO-PEG400 and CuO-PEG6000 respectively, in water medium at 303.15 K.

Download CSV Display Table

Table 3: Limiting density ($\rho°$, kg m^{-3}), 1st degree slope (S_ρ, kg^{2}m^{-3}mol^{-1}), Limiting apparent molar volume, ($V_\phi°$, m^3·mol^{-1}), 1st degree slope ($S_{V\phi}$, kg$^{1/2}$·m^3·mol$^{-3/2}$), Limiting refractive index (µri °), 1st degree slope ($S_{\mu ri}$), Limiting molar refraction (R°, cm^{3}mol^{-1}), 1st degree slope (S_R, cm^3 mol^{-1})

Download CSV Display Table

These compositions support the dispersion activities of CuO NPs in water, PEG_{400} and PEG_{6000}, which is strong with increasing densities due structural activities show higher interactions. The

In this article

higher structure breaking effects in water as compared to PEG. This confirmed the domination of hydrophobic chain on dispersion activities of CuO NPs as water shows hydrophilic nature as compared to PEG.

3.4. Apparent Molar Volume (V_ϕ)

The apparent molar volume, V_ϕ ($m^3 \cdot mol^{-1}$) was calculated by using densities data with following equation:

$$V_\Phi = \frac{1000\left(\rho^0 - \rho\right)}{m\rho^0\rho} + \frac{M}{\rho} \quad (2)$$

where $\rho°$ and ρ are the densities of the water and solutions (PEG400-W, PEG6000-W, CuO-W, CuO-PEG_{400} and CuO-PEG_{6000}) respectively, m (10^{-6} mol/L) is the molarity of solute (CuO, PEG_{400} and PEG_{6000}) and M ($kg \cdot mol^{-1}$) is the molar mass of solute. The V_ϕ data were regressed for limiting apparent molar volume ($V_\phi°$) and obtained by fitting the values in equation as given below:

$$V_\Phi = V_\Phi^\circ + S_v m^{1/2} + B_v\, m \quad (3)$$

where $V_\phi°$ represents the state of solute–solvent intermolecular interaction, while S_v ($kg^{1/2} \cdot m^3 \cdot mol^{-3/2}$) and B_v ($kg \cdot m^3 \cdot mol^{-2}$) are 1st and 2nd degree slopes and facilitated to evaluate solute–solute interactions [26] (Table 3). The V_ϕ and $V_\phi°$ values are given in Tables 2 and 3 and shown in Figure 3a,b.

Figure 3. Apparent molar volume of (a) PEG400-W and PEG6000-W (b) CuO-W, Cu-PEG400, CuO-PEG6000.

In this article

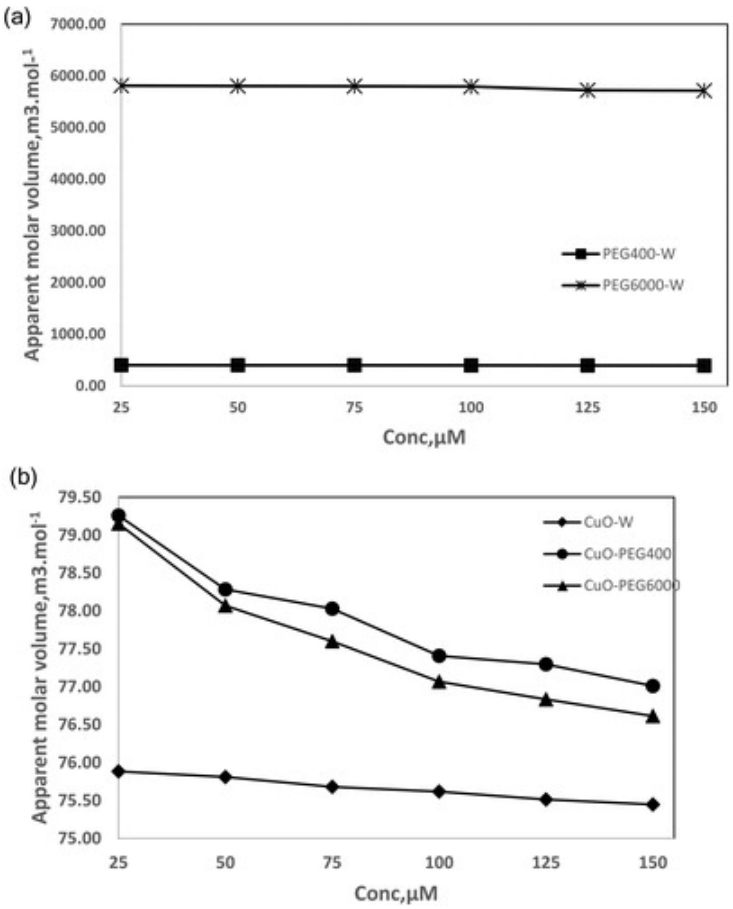

Display full size

The V_ϕ values decreased with increasing concentration of CuO NPs, depicting increased hydrophobic forces in the dispersion solution due to presence of hydrophobic chain in polymer. Though, this reason is absent in water because of dipoles introduces hydrophilicity and initiate the dispersion activities. The limiting V_ϕ values with order CuO-PEG_{400} > CuO-PEG_{6000} > CuO-W revealed that the minimum V_ϕ in hydrophobicity of PEG_{400}, may have induced reorientation of the CuO molecules with PEG_{400} as compared to PEG6000 (Table 3, Figure 3a).

The increase in limiting V_ϕ values with PEG400 in water is due to increased solute–solvent interactions. This may be due to the increased hydrophobic and hydrophilic interaction between CuO and PEG_{400}, which weaken the dipole–dipole interaction between CuO NPs and water.

Lower limiting $V\phi$ values showed with water may be due to the dominance of hydrophilic and repulsive forces (Cu^{2+} and O^- ion of CuO NPs) on the ion–dipole interaction with enhancing CuO NPs concentration in water molecule. This infers that the electrostatic interaction between CuO

In this article

3.5. Refractive Index, Molar Refraction and Speed of Light

The refractive index was determined with Abbe Refractometer. All samples were measure refractive index and it is calibrated by Distilled Water. To understand state of polarizability, the molar refraction is chemical and constitutive property and was calculated with Lorentz–Lorenz Eq. (4) [27] as given below.

$$R = \frac{\mu^2{}_{ri} - 1}{\mu^2{}_{ri} + 2} x \ \frac{M}{\rho} \quad (4)$$

The M is the molecular mass, ρ is density and μ_{ri} is the refractive index. The calculated molar refraction (R) depend on the concentration of substance entangled in solution [28]. The speed of light, C was calculated with following equation and given in Table 2,

$$C = \frac{3 \times 10^8}{\mu_{ri}} \quad (5)$$

The 3×10^8 m s^{-1} value depicts light velocity in vacuum and μ_{ri} is the refractive index.

The PCPs can be correlated with the absorbance values of the binary systems.

The molecular dispersion based on the molecular reorientation and number of molecules which can have determined with speed of light in vacuum and medium. The μ_{ri} of pure W and PEGs are agree with literature [25, 29] as shown in Table 1. The μ_{ri} values for PEG_{400}-W, PEG_{6000}-W, CuO-W, CuO-PEG_{400} and CuO-PEG_{6000} presented in Table 2 and Figure 4. These results show μ_{ri} increased with increasing concentration of PEG_{400}, PEG_{6000} and CuO in water (Table 2). The limiting μ_{ri} of PEG6000 is higher by 0.0008 as compared to PEG400 which inferred the slightly activity of hydrophobic chain on refractive properties.

Figure 4. Refractive index of CuO, PEG400, PEG6000, CuO-PEG400 and CuO-PEG6000 in water.

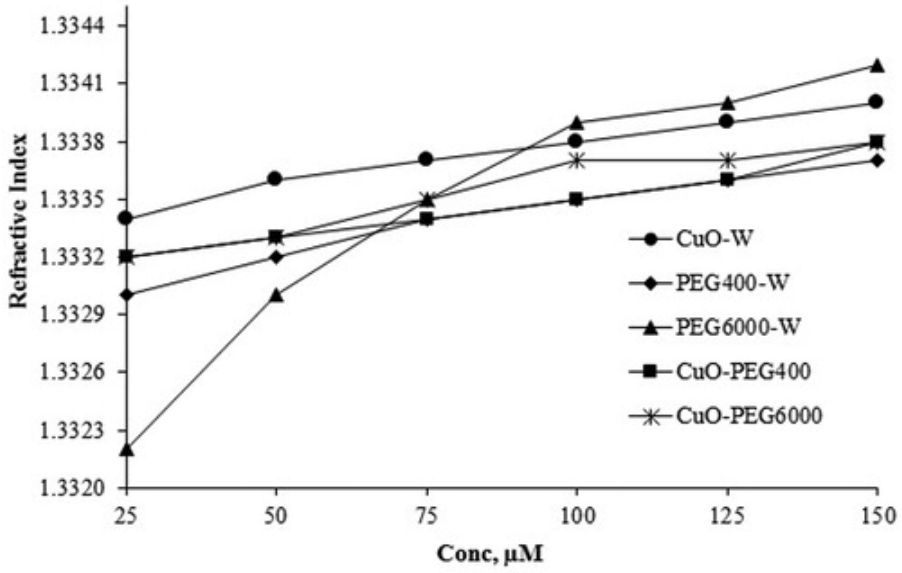

Display full size

The limiting μ_{ri} values in terms of composition of dispersed CuO NPs follows the order as CuO-PEG400 = CuOPEG6000 > CuO-W (Table 2). This infers with molecular alignment, the compacted medium due to hydrophobic and hydrophilic centers, provides a restricted pathway for the passing of light waves. Without hydrophobic centers, especially in case of CuO-W the passing pathways becomes movable and also confirmed the weaker involvement of hydrophilic domains in the systems during passing light. The refractive index (Figure 4), speed of light (Figure 5) and molar refraction (Figure 6) result inferred that dipoles, hydrophobic-hydrophilic interactions and composition of the CuO which slightly influence the refraction properties.

Figure 5. Speed of light of CuO, PEG400, PEG6000, CuO-PEG400 and CuO-PEG6000 in water.

In this article

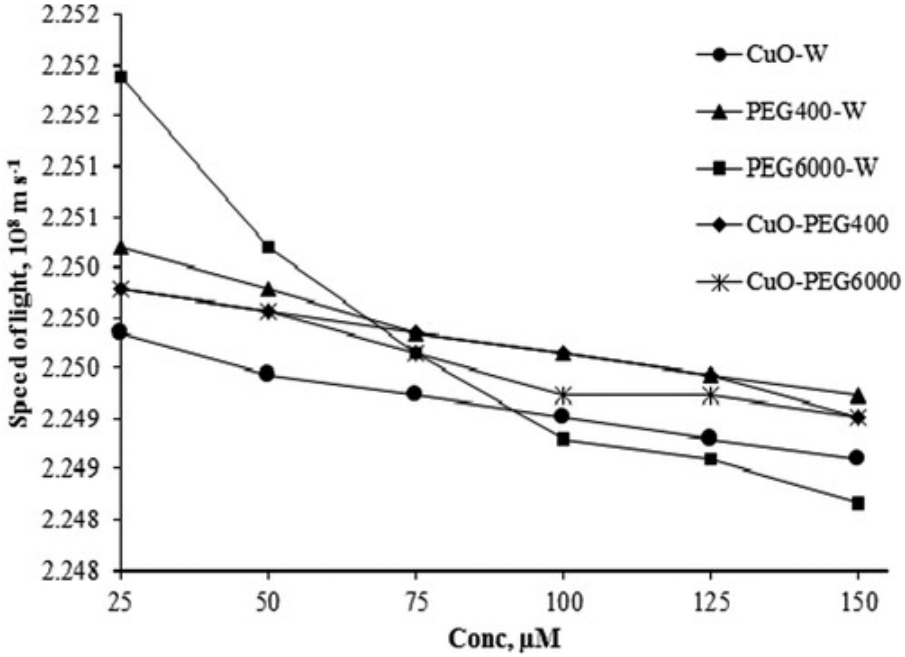

Display full size

Figure 6. Molar refraction of (a) PEG400, PEG6000, (b) CuO, CuO-PEG400, CuO-PEG6000 in water.

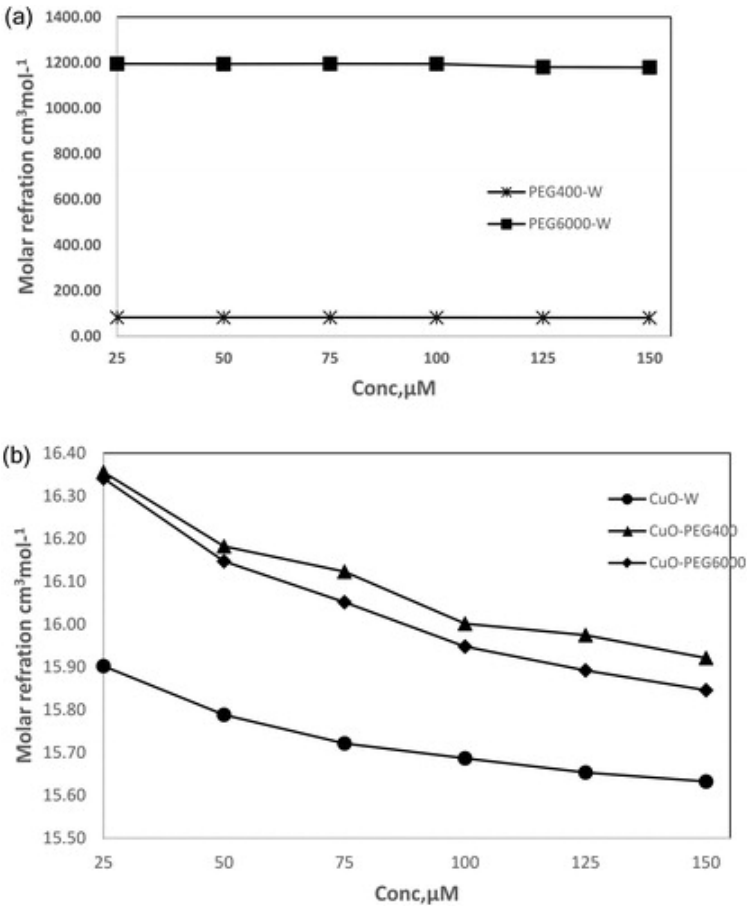

In this article

3.6. pH Studies

The pH of PEG_{400}-W, PEG_{6000}-W, CuO-W, CuO-PEG_{400} and CuO-PEG_{6000} are given in Table 2, where pH found in the range 7–8 in all systems which releveled a presence of [sbond]OH and H^+. The structural networks of these dispersion systems are the sources for interactions that are restrained through [sbond]OH of PEG and ($H^{\delta+}$[sbond]$O^{\delta-}$[sbond]$H^{\delta+}$) of water molecules. In general, pH of attributed to the acidic and basic nature along with kinetic energy encouraged higher H^+ generation in the solution. In this study, the pH showed slightly dissimilar variations towards basic nature for PEG_{400}-W, PEG_{6000}-W, CuO-W, CuO-PEG_{400} and CuO-PEG_{6000}. This revealed that in solutions have only water dipole may be for H^+ generating sources whereas, the PEG have additional [sbond]OH which restricted the H^+ common dissociation activities. Despite, the all systems developed slightly higher >7 pH than only water. Furthermore, there are huge potentials to neutralize the H + in the dispersion systems which maintained within range 7–8 pH (Table 2, Figure 7). These results also confirm the formation of hydrogen bond breaking systems in the in water during dispersion of CuO NPs by using polymeric structure. Thus, influence stability of dispersed CuO in water and PEG by Lewis acid base conjugate potentials with H + involvement in water.

Figure 7. pH of CuO, PEG400, PEG6000, CuO-PEG400 and CuO-PEG6000 in water.

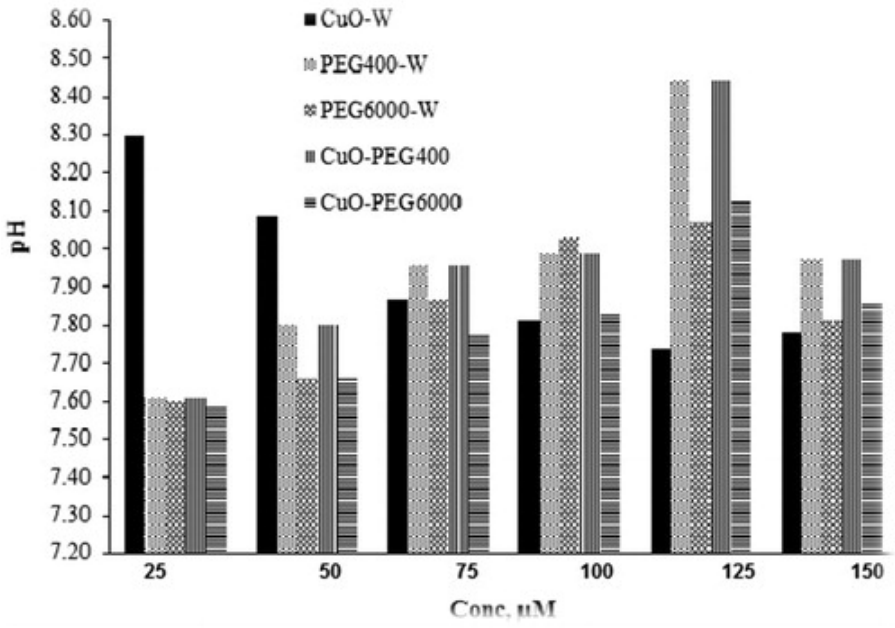

Display full size

In this article

Figures 8 and 9, show the UV-Vis spectra for all dispersed systems. The optical absorption spectra for cupric NP with PEG 400 and W increased with increased concentration (25–150) μM. The absorbance peaks are 373, 375, 376.5, 377, 378 and 379 nm, which are correspond to red shift (bathochromic and hyperchromic) [29]. This is indicating to dispersive activity for CuO NPs and 150 μM have high dispersed than others as show in Figure 8a. The red shift is may be referring to a number of oxygen vacancies in CuO, also may to present of a small amount of Cu^{2+} ions on the surface. This strong absorption in range (200–400) nm because of charge transfer transition from 2p-orbital of O^{2-} to the 3d-orbital of Cu^{2+} in CuO [30]. In binary PEG400 + W and PEG6000 + W, UV-Vis spectra of this system were recorded and optical spectra show in Figure 8b,c.

Figure 8. **(a)** UV-Vis absorbance spectra of 25 μM to 150 μM CuO in water. **(b)** UV-Vis absorbance spectra of 25 μM to 150 μM PEG400 in water. **(c)** UV-Vis absorbance spectra of 25 μM to 150 μM PEG6000 in water. **(d)** UV-Vis absorbance spectra of 25 μM to 150 μM CuO in 150 μM aqueous PEG400. **(e)** UV-Vis absorbance spectra of 25 μM to 150 μM CuO in 150 μM aqueous PEG6000.

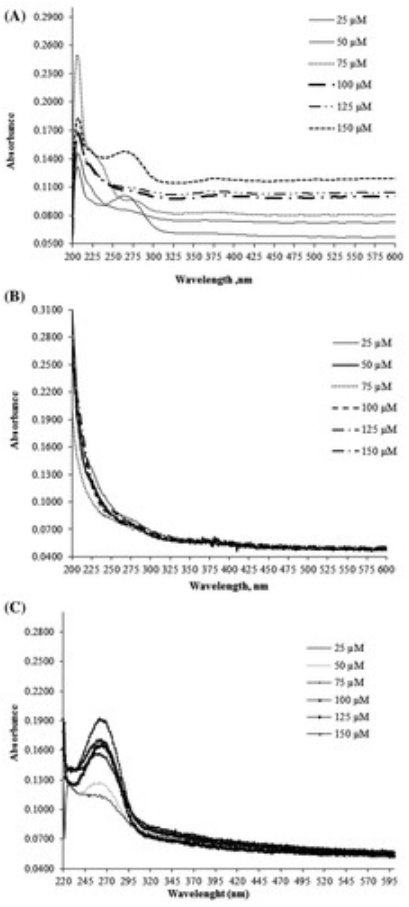

Display full size

In this article

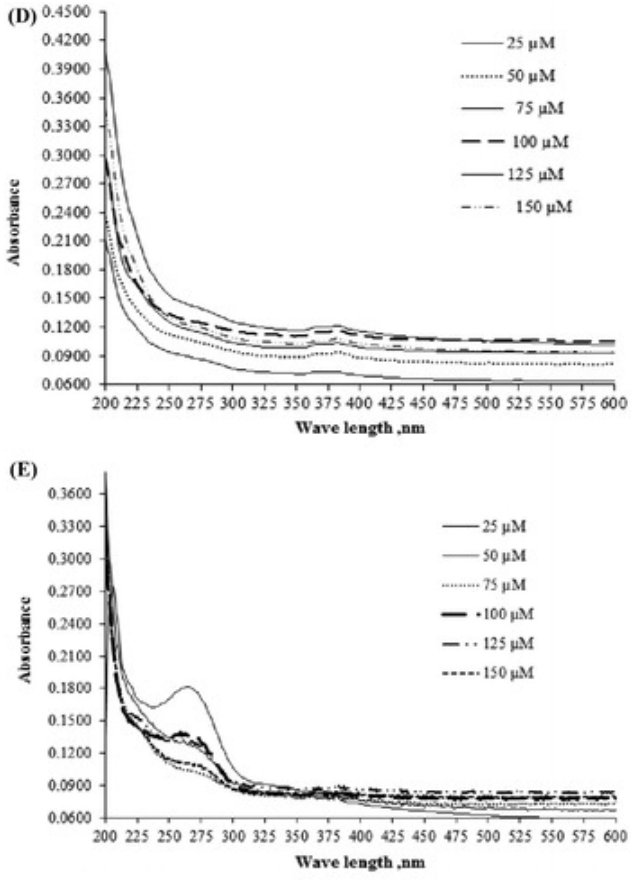

Display full size

Figure 9. The absorbance (A,±10^{-3}) at λmax 207, 268, 269, 273 and 265 nm with concentration 25–150 µM of CuO, PEG400, PEG6000 and CuO-PEG400 and CuO-PEG6000 respectively, in water at 303.15 K.

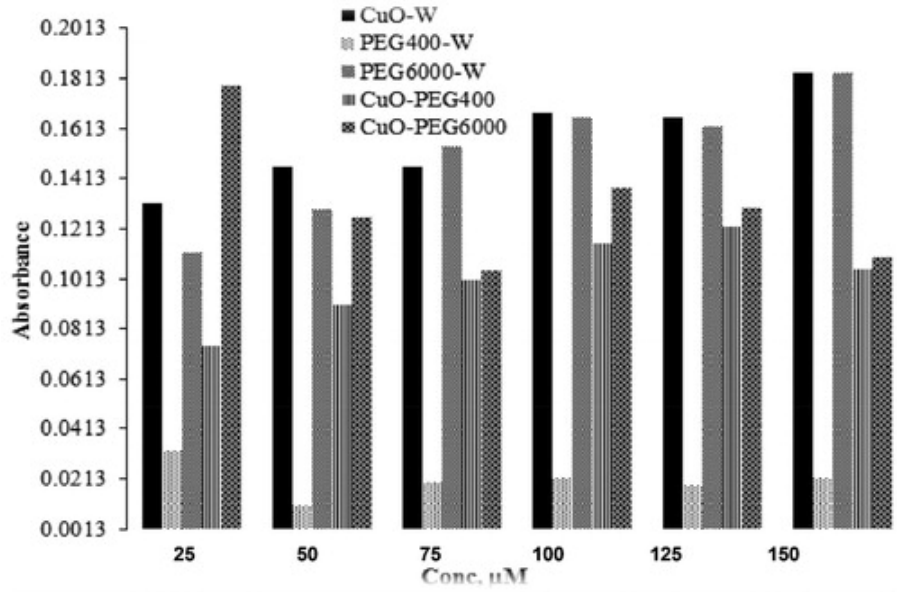

In this article

The CuO, PEG_{400} and PEG_{6000} separately showed a lower absorbance in aqueous medium as compared to CuO with both PEG in aqueous medium as shown in Figure 8d,e. The optical properties also confirmed the dispersion activity of CuO NPs with polymeric formulations. All optical absorbance of binary and ternary system shown in Figure 9.

4. Conclusions

In this study we used of MONP and their dispersion activities physiochemical and optical properties of this nanoparticle. The results confirmed the CuO nanoparticles have a good dispersion potential in aqueous and polymeric solutions. The density and refractive index are increases by in increase the chain length of PEGs and also increase with dipoles of water molecule. The PEG400 and PEG6000 having a hydrophobic alkyl chain ([sbond]CH_2[sbond]CH_2[sbond])$_n$ and hydrophilic [sbond]OH groups which contribute for accommodation of CuO NPs in water medium through molecular interactions as per structural activities. Our study with such significant results shows higher structural activities to develop various biological, environmental and human health applications and new approach for enhancing the dispersion of CuO NPs.

Acknowledgements

The authors are thankful to the UGC-SAP, New Delhi, India.

References

1. A. J. Lewis, Colloidal processing of ceramics, *J. Am. Ceram. Soc.* **83** (10), 2341 (2004). DOI: 10.1111/j.1151-2916.2000.tb01560.x.
   Google Scholar

agglomeration state of nanoparticle dispersions for toxicological studies, *J. Nanopart. Res.* **11**, 77 (2009). DOI: 10.1007/s11051-008-9446-4.

Web of Science ® | Google Scholar

3. K. Hidehiro and M. Lijima, Surface modification and characterization for dispersion stability of inorganic nanometer-scaled particles in liquid media, *Sci. Technol. Adv. Mater.* **11**, 044304 (2010).

PubMed | Web of Science ® | Google Scholar

4. V. Donna, C. Tom, and N. K. Chandar, Effect of CTAB on structural and optical properties of CuO nanoparticles prepared by coprecipitation route, presented at the IOP Conference Series: Materials Science and Engineering, 2017, Vol. 263.

Google Scholar

5. A. A. Radhakrishnan and B. B. Beena, Structural and optical absorption analysis of CuO nanoparticles, *Indian J. Adv. Chem. Sci.* **2**, 158 (2014).

Google Scholar

6. W. Wang et al., A simple wet-chemical synthesis and characterization of CuO nanorods, *Appl. Phys. A: Mater. Sci. Process* **76** (3), 417 (2003). DOI: 10.1007/s00339-002-1514-5.

Web of Science ® | Google Scholar

7. W. Dangxin, Q. Zhang, and M. Tao, LSDA + U study of cupric oxide: Electronic structure and native point defects. *Phys. Rev. B* **73** (23), 235206 (2006). DOI: 10.1103/PhysRevB.73.235206.

Web of Science ® | Google Scholar

8. L. Dongdong et al., Conductometric chemical sensor based on individual CuO nanowires, *Nanotechnology* **21**, 485502 (2010). DOI: 10.1088/0957-4484/21/48/485502.

PubMed | Web of Science ® | Google Scholar

9. S. Felix, R. B. P. Chakkravarthy, and A. N. Grace, Microwave assisted synthesis of copper oxide and its application in electrochemical sensing, presented at the IOP Conference Series:

In this article

Google Scholar

10. M. Shahmiri et al., Preparation of PVP-coated copper oxide nanosheets as antibacterial and antifungal agents, *J. Mater. Res.* **28** (22), 3109 (2013). DOI: 10.1557/jmr.2013.316.
Web of Science ® | Google Scholar

11. L. Cheng et al., Preparation, characterization, and electrochemical application of mesoporous copper oxide, *Mater. Res. Bull.* **45** (2), 235 (2010). DOI: 10.1016/j.materresbull.2009.08.001.
Web of Science ® | Google Scholar

12. F. B. Tehrani, S. I. Vasefi, and A.M. Anvari, Analysis of particle dispersion and entropy generation in turbulent mixed convection of CuO-water nanofluid, *Heat Transf. Eng.* **40** (1–2), 81 (2019). DOI: 10.1080/01457632.2017.1404828.
Web of Science ® | Google Scholar

13. Y. N. Chang et al., The toxic effects and mechanisms of CuO and ZnO nanoparticles, J. *Mater.* **5** (12), 2850 (2012). DOI: 10.3390/ma5122850.
Google Scholar

14. V. Rajput et al., ZnO and CuO nanoparticles: A threat to soil organisms, plants, and human health, *Environ. Geochem. Health* **1–12** (2019).
Google Scholar

15. L. Kai, H. Jiang, and Q. Zhang, A colorimetric method for the molecular weight determination of polyethylene glycol using gold nanoparticles, *Nanoscale Res. Lett.* **8**, 538 (2013). DOI: 10.1186/1556-276X-8-538.
PubMed | Web of Science ® | Google Scholar

16. H. J. Milton, ed. *Poly (Ethylene Glycol) Chemistry: Biotechnical and Biomedical Applications* (Springer Science & Business Media, Berlin, Germany, 2013).
Google Scholar

In this article

17. Duncan, Ruth, "Polymer conjugates as anticancer nanomedicines." *Nat. Rev. Cancer* **6.9**, 688 (2006). DOI: 10.1038/nrc1958.

Google Scholar

18. S. Sh and A. Jouyban, Solubility of lamotrigine in binary and ternary mixtures of PEGs 200, 400, and 600 with ethanol, PG, and water at 298.2 K, *Chem. Eng. Commun. 200* (11), 1443 (2013). DOI: 10.1080/00986445.2012.751378.

Web of Science ® | Google Scholar

19. T. Shruti, C. Bhanot, and S. Pandey, Densities of {poly (ethylene glycol) + water} over the temperature range (283.15 to 363.15) K, *J. Chem. Thermodyn.* **42**, 1367 (2010). DOI: 10.1016/j.jct.2010.06.001.

Web of Science ® | Google Scholar

20. P.-Å. Albertsson, Partition of cell particles and macromolecules in polymer two-phase systems, *Adv. Protein Chem.* **24**, 309 (1970).

PubMed | Google Scholar

21. B. E. Poling et al., *Perry's Chemical Engineers' Handbook* (McGraw-Hill Publishing, New York, NY, 2008).

Google Scholar

22. Z. Kolská et al., Study of binary system glycerine–water and its colloidal samples of silver nanoparticles, *J. Mol. Liq. 218*, 363 (2016). DOI: 10.1016/j.molliq.2016.02.063.

Web of Science ® | Google Scholar

23. D. Masahiko and A. Masumura, Measurement of the refractive index of distilled water from the near-infrared region to the ultraviolet region, *Appl. Opt.* **46**, 3811 (2007). DOI: 10.1364/AO.46.003811.

PubMed | Web of Science ® | Google Scholar

24. D. R. Lide and T. J. Bruno, *CRC Handbook of Chemistry and Physics* (CRC Press LLC, Boca Raton

In this article

Google Scholar

25. S. B. Undre, M. Singh, and R. K. Kale, Interaction behaviour of trimesoyl chloride derived 1st tier dendrimers determined with structural and physicochemical properties required for drug designing, *J. Mol. Liq.* **182**, 106 (2013). DOI: 10.1016/j.molliq.2013.03.019.

Web of Science ® | Google Scholar

26. N. Vashistha, A. Chandra, and M. Singh, Influence of rhodamine B on interaction behaviour of lanthanide nitrates with 1st tier dendrimer in aqueous DMSO: A physicochemical, critical aggregation concentration and antioxidant activity study, *J. Mol. Liq.* **260**, 323 (2018). DOI: 10.1016/j.molliq.2018.03.056.

Web of Science ® | Google Scholar

27. A. Z. Tasic et al., Use of mixing rules in predicting refractive indexes and specific refractivities for some binary liquid mixtures, *J. Chem. Eng. Data* **37** (3), 310 (1992). DOI: 10.1021/je00007a009.

Web of Science ® | Google Scholar

28. R. K. Ameta, M. Singh, and R. K. Kale, Comparative study of density, sound velocity and refractive index for (water + alkali metal) phosphates aqueous systems at T = (298.15, 303.15, and 308.15 K, *J. Chem. Thermodyn.* **60**, 159 (2013). DOI: 10.1016/j.jct.2013.01.012.

Web of Science ® | Google Scholar

29. D. Seo, J. Park, T. Shin, P. Yoo, J. Park, K. and Kwak, Bathochromic shift in absorption spectra of conjugated polymer nanoparticles with displacement along backbones. *Macromolecular Research*, *23*, 574–577.(2015) DOI: 10.1007/s13233-015-3078-1.

Web of Science ® | Google Scholar

30. K. Khashan, S., M. Jabir S., and F. Abdulameer, A., Preparation and characterization of copper oxide nanoparticles decorated carbon nanoparticles using laser ablation in liquid. *In Journal of Physics: Conference Series* (Vol. 1003, No. 1, p. 012100). IOP Publishing.(2018) DOI: 10.1088/1742-6596/1003/1/012100

In this article